

Chemical Kinetic Reaction Mechanism for the Combustion of Propane

CASIMIR J. JACHIMOWSKI

NASA Langley Research Center, Hampton, Virginia 23665

A detailed chemical kinetic reaction mechanism for the combustion of propane is presented and discussed. The mechanism consists of 27 chemical species and 83 elementary chemical reactions. Ignition and combustion data as determined in shock tube studies were used to evaluate the mechanism. Numerical simulation of the shock tube experiments showed that the kinetic behavior predicted by the mechanism for stoichiometric mixtures is in good agreement with the experimental results over the entire temperature range examined (1150–2600K). Sensitivity and theoretical studies carried out using the mechanism revealed that hydrocarbon reactions which are involved in the formation of the HO_2 radical and the H_2O_2 molecule are very important in the mechanism and that the observed nonlinear behavior of ignition delay time with decreasing temperature can be interpreted in terms of the increased importance of the HO_2 and H_2O_2 reactions at the lower temperatures.

INTRODUCTION

Recent interest in cruise missile development has generated interest in the possible use of a hydrocarbon fueled scramjet as the propulsion unit. As this interest grows it is anticipated that reaction models will become valuable tools in the study of the supersonic combustion of hydrocarbon fuels in the same way that reaction models have been used to study the supersonic combustion of hydrogen.

Even though the kinetics and mechanisms of hydrocarbon combustion have been studied for many years, the reaction and rate coefficient data base is insufficient to assemble reaction mechanisms describing the combustion of practical hydrocarbon fuels such as jet fuels and ramjet fuels. Detailed mechanisms have been assembled and applied for only the simplest of hydrocarbons, such as methane, ethane, acetylene, ethylene, methanol, and to a limited extent propane. An attempt to model comprehensively the combustion of complex practical fuels would be highly speculative and the computed results obtained with the model would be suspect. It is generally accepted, however, that

propane is the simplest hydrocarbon which has reaction characteristics that are typical of many practical hydrocarbon fuels, including jet fuels and ramjet fuels. Therefore, from a modeling perspective, a propane combustion mechanism which has been assembled and evaluated against experimental data would be a valuable research tool for analyzing and interpreting supersonic combustion experiments involving typical hydrocarbon fuels. This mechanism would be especially valuable in connection with experiments in which propane was used as a surrogate hydrocarbon fuel.

In this paper a detailed chemical kinetic mechanism for the combustion of propane is presented and discussed. The mechanism is essentially an expanded version of the propane mechanism previously proposed by McLain and Jachimowski [1] and applied to the study of nitric oxide formation in jet stirred combustors [2]. In the mechanism the propane was assumed to pyrolyze rapidly and react to form lower molecular weight products, such as ethylene, methane, and propylene, followed by the oxidation of these hydrocarbon products. The mechanism was refined by comparing the observed kinetic behavior as

determined in shock tube studies with that predicted by the mechanism. To obtain good agreement between experimental and calculated results, rate coefficients for several reactions had to be adjusted. The mechanism was developed primarily to describe the high temperature ($T > 1400\text{K}$) combustion of propane and was unable to predict the observed kinetic behavior at the lower temperatures ($T < 1300\text{K}$).

The mechanism presented in this paper incorporates recent mechanistic and kinetic information on the pyrolysis and oxidation of propane and its pyrolysis products. Also, reactions which were likely to be important at the lower temperatures, especially reactions which produce and consume the HO_2 radical and H_2O_2 , were included in the mechanism. The resulting propane combustion mechanism was evaluated by comparing calculated results with experimental results on the ignition and oxidation of stoichiometric propane mixtures behind shock waves [1, 3].

PROPANE COMBUSTION MECHANISM

The proposed propane combustion scheme, even though it contains many reactions, is still a rather simplified mechanism in that only the major reaction products are considered. Recent experimental results obtained by Hautmann et. al. [4] on the oxidation of propane in a high temperature, turbulent flow reactor showed that the major intermediate hydrocarbon products are primarily olefinic, the largest fraction being composed of ethylene and propylene. Other intermediates, including oxygenated hydrocarbons, were detected; however, the quantities were substantially smaller than the major intermediates. Consequently, reactions involving species such as allene, propyne, acetone, acetaldehyde, etc., are not included in the mechanism. The proposed propane combustion mechanism and the reaction rate coefficients are listed in Table 1.

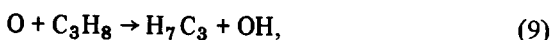
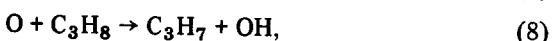
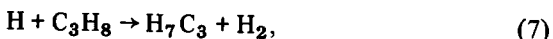
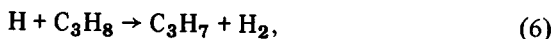
When the original oxidation mechanism [1] was assembled it was necessary to estimate the rate coefficients for the propane decomposition reaction because sufficient kinetic data were not available. Recently Chiang and Skinner [5] investigated the decomposition of propane behind reflected shock

waves over the temperature range 1200-1450K for pressures between 2 to 3 atm. They reported the rate coefficient $k = 2.5 \times 10^{16} \exp(-87,500/RT) \text{ s}^{-1}$ for the reaction



Tsang [6], who studied the decomposition of propane using the single shock tube technique, reported the high pressure first order rate coefficient $k_\infty = 4 \times 10^{16} \exp(-84800/RT) \text{ s}^{-1}$. Using the RRK theory for unimolecular reactions and the RRK estimation methods proposed by Golden et al. [7], in which the effective number of oscillators is determined by the vibrational heat capacity [$s \equiv (C_p - 4R)/R$], it was determined that the Chiang and Skinner and the Tsang rate coefficients are consistent with each other if the RRK collision efficiency λ is set at 10^{-3} . The propane decomposition rate coefficient used in the mechanism is the high pressure rate coefficient reported by Tsang. RRK theory [7] with λ set at 10^{-3} was used to obtain the rate coefficients at other pressures. The rate coefficients selected for the decomposition of the propyl radicals ($\text{C}_3\text{H}_7 = n\text{-propyl}$, $\text{H}_7\text{C}_3 = i\text{-propyl}$) and the ethyl radical, reactions 14, 16, 17, and 26, were obtained in a similar manner using the high pressure rate coefficients recommended by Lifshitz and Frenklach [8] and Benson and O'Neal [9] with λ set at 10^{-3} . The selection of λ as 10^{-3} for these reactions is based totally on analogy with the propane decomposition reaction and may be questionable. However, comparison of the results of subsequent calculations with experimental data showed that the calculated results were not very sensitive to the rates of these reactions.

The rate coefficients for the abstraction of a hydrogen atom from propane by the hydrogen and oxygen atoms,



were obtained using the overall rate coefficients

TABLE 1

Propane Combustion Mechanism Rate Coefficients in cm³ mole s kcal Units: $k = AT^n \exp(-E/RT)$

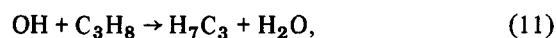
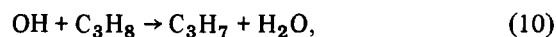
Reaction	log A	n	E	Reference
1 C ₃ H ₈ → C ₂ H ₅ + CH ₃	16.6	0	84.8	5
2 ^a C ₃ H ₈ + O ₂ → C ₃ H ₇ + HO ₂	13.0	0	52.0	Estimated
3 ^a C ₃ H ₈ + O ₂ → H ₇ C ₃ + HO ₂	12.5	0	52.0	$k_3 = \frac{1}{3}k_2$
4 CH ₃ + C ₃ H ₈ → C ₃ H ₇ + CH ₄	12.5	0	11.4	8
5 CH ₃ + C ₃ H ₈ → H ₇ C ₃ + CH ₄	11.9	0	8.6	8
6 H + C ₃ H ₈ → C ₃ H ₇ + H ₂	13.7	0	9.1	8
7 H + C ₃ H ₈ → H ₇ C ₃ + H ₂	13.1	0	6.4	8
8 O + C ₃ H ₈ → C ₃ H ₇ + OH	13.6	0	11.1	1
9 O + C ₃ H ₈ → H ₇ C ₃ + OH	13.0	0	8.4	1
10 OH + C ₃ H ₈ → C ₃ H ₇ + H ₂ O	4.7	2.7	0.1	10
11 OH + C ₃ H ₈ → H ₇ C ₃ + H ₂ O	3.7	2.8	-1.7	10
12 HO ₂ + C ₃ H ₈ → C ₃ H ₇ + H ₂ O ₂	11.8	0	10.5	$k_{12} = 3k_{13}$
13 HO ₂ + C ₃ H ₈ → H ₇ C ₃ + H ₂ O ₂	11.3	0	10.5	15
14 C ₃ H ₇ → C ₂ H ₄ + CH ₃	13.6	0	33.2	9
15 H ₇ C ₃ → C ₂ H ₄ + CH ₃	12.0	0	34.5	8
16 C ₃ H ₇ → C ₃ H ₆ + H	13.8	0	38.0	9
17 H ₇ C ₃ → C ₃ H ₆ + H	14.3	0	41.3	9
18 C ₃ H ₇ + O ₂ → C ₃ H ₆ + HO ₂	12.0	0	5.0	$k_{18} = k_{42}$
19 H ₇ C ₃ + O ₂ → C ₃ H ₆ + HO ₂	12.0	0	5.0	$k_{19} = k_{42}$
20 CH ₃ + C ₃ H ₆ → C ₃ H ₅ + CH ₄	12.4	0	5.4	13
21 H + C ₃ H ₆ → C ₂ H ₄ + CH ₃	12.6	0	0	16
22 H + C ₃ H ₆ → C ₃ H ₅ + H ₂	13.7	0	5.0	13
23 OH + C ₃ H ₅ → C ₂ H ₄ + CH ₂ O	13.0	0	0	Estimated
24 O + C ₃ H ₆ → C ₂ H ₅ + HCO	13.4	0	2.7	$k_{24} = k_{47}$
25 OH + C ₃ H ₆ → C ₂ H ₅ + CH ₂ O	13.0	0	0	Estimated
26 C ₂ H ₅ → C ₂ H ₄ + H	13.5	0	40.7	9
27 M + CH ₄ → CH ₃ + H + M	17.1	0	88.4	17
28 H + CH ₄ → CH ₃ + H ₂	14.8	0	15.1	18
29 O + CH ₄ → CH ₃ + OH	14.6	0	14.0	18
30 OH + CH ₄ → CH ₃ + H ₂ O	13.5	0	6.0	19
31 CH ₃ + O → CH ₂ O + H	14.1	0	2.0	19
32 CH ₃ + O ₂ → CH ₃ O + O	13.4	0	29.0	20
33 CH ₃ + HO ₂ → CH ₃ O + OH	13.2	0	0	13
34 CH ₃ + OH → CH ₂ O + H ₂	12.6	0	0	13
35 M + CH ₃ O → CH ₂ O + H	13.7	0	21.0	20
36 CH ₃ O + O ₂ → CH ₂ O + HO ₂	12.0	0	6.0	13
37 CH ₃ + CH ₃ → C ₂ H ₆	12.8	0	-1.0	21
38 CH ₃ + C ₂ H ₆ → C ₂ H ₅ + CH ₄	-0.3	4.0	8.3	13
39 H + C ₂ H ₆ → C ₂ H ₅ + H ₂	7.5	2.0	6.9	21
40 O + C ₂ H ₆ → C ₂ H ₅ + OH	13.2	0	6.1	22
41 OH + C ₂ H ₆ → C ₂ H ₅ + H ₂ O	13.8	0	3.6	22
42 HO ₂ + C ₂ H ₆ → C ₂ H ₅ + H ₂ O ₂	12.0	0	14.0	15
43 C ₂ H ₅ + O ₂ → C ₂ H ₄ + HO ₂	12.0	0	5.0	13
44 H + C ₂ H ₅ → 2 CH ₃	13.0	0	0	21
45 H + C ₂ H ₅ → H ₂ + C ₂ H ₄	13.7	0	0	18
46 H + C ₂ H ₄ → C ₂ H ₃ + H ₂	14.0	0	8.5	19
47 O + C ₂ H ₄ → CH ₃ + HCO	13.4	0	2.7	19
48 OH + C ₂ H ₄ → C ₂ H ₃ + H ₂ O	14.0	0	3.5	19
49 M + C ₂ H ₃ → C ₂ H ₂ + H + M	14.9	0	31.5	23
50 H + C ₂ H ₂ → C ₂ H + H ₂	14.3	0	19.0	24
51 O + C ₂ H ₂ → CH ₂ + CO	13.7	0	3.7	23

TABLE 1 (Continued)

	Reaction	log <i>A</i>	<i>n</i>	<i>E</i>	Reference
52	OH + C ₂ H ₂ → C ₂ H + H ₂ O	12.8	0	7.0	24
53	C ₂ H + O ₂ → HCO + CO	13.0	0	7.0	19
54	CH ₂ + O ₂ → HCO + OH	14.0	0	3.7	19
55	H + CH ₂ O → HCO + H ₂	14.5	0	10.5	25
56	O + CH ₂ O → HCO + OH	13.3	0	3.1	25
57	OH + CH ₂ O → HCO + H ₂ O	12.9	0	0.2	25
58	HO ₂ + CH ₂ O → HCO + H ₂ O ₂	12.1	0	8.0	15
59	M + HCO → CO + H + M	14.7	0	19.0	26
60	H + HCO → CO + H ₂	14.3	0	0	25
61	O + HCO → CO + OH	14.0	0	0	25
62	OH + HCO → CO + H ₂ O	14.0	0	0	25
63	HCO + O ₂ → CO + HO ₂	12.5	0	7.0	30
64	OH + CO → CO ₂ + H	7.2	1.3	-0.7	27
65	HO ₂ + CO → CO ₂ + OH	14.2	0	23.6	21
66	CO + O + M → CO ₂ + M	15.4	0	4.4	21
67	H + O ₂ → OH + O	17.1	-0.9	16.6	29
68	OH + H ₂ → H ₂ O + H	7.5	1.8	3.0	29
69	O + H ₂ → OH + H	14.3	0	13.8	28
70	OH + OH → H ₂ O + O	13.7	0	7.0	29
71	H + OH + M → H ₂ O + M	22.3	-2.0	0	30
72	H + H + M → H ₂ + M	17.8	-1.0	0	30
73	H + O ₂ + M → HO ₂ + M	18.5	-1.0	0	31
74	OH + HO ₂ → H ₂ O + O ₂	13.7	0	1.0	15
75	H + HO ₂ → H ₂ + O ₂	13.4	0	0.7	15
76	H + HO ₂ → 2 OH	14.7	0	1.8	15
77	O + HO ₂ → OH + O ₂	13.7	0	1.0	15
78	HO ₂ + HO ₂ → H ₂ O ₂ + O ₂	12.3	0	0	31
79	HO ₂ + H ₂ → H ₂ O ₂ + H	11.5	0	18.7	31
80	OH + H ₂ O ₂ → HO ₂ + H ₂ O	13.0	0	1.9	30
81	M + H ₂ O ₂ → 2 OH + M	17.1	0	45.5	30
82	H + H ₂ O ₂ → H ₂ O + OH	12.7	0	9.9	30
83	O + H ₂ O ₂ → HO ₂ + OH	13.3	0	5.9	30

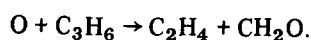
^a C₃H₇ = normal propyl radical; H₇C₃ = isopropyl radical.

[1, 8] and the function $k_i/k_n = 0.24 \exp(2700/RT)$ recommended by Lifshitz and Frenklach [8]. In the previous propane mechanism [1], differences in the rate coefficients for the formation of the iso and normal forms of the propyl radical were not considered. The rate coefficients for the abstraction of a hydrogen atom from propane by the hydroxyl radical,



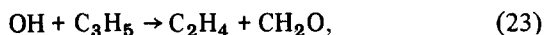
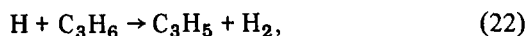
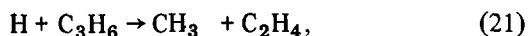
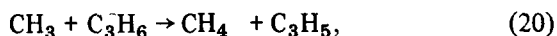
were taken from Cohen [10], who used transition state theory to extrapolate existing experimental data to higher temperatures.

The reactions and rate coefficients that were used to describe the oxidation of methane, ethylene, acetylene, and ethane were based for the most part on the mechanisms tested and reported by Westbrook [14], Olson and Gardiner [22], and Jachimowski [26]. Due to the lack of adequate kinetic data on the high temperature oxidation of propylene, the consumption of propylene in the original propane mechanism [1] was described by the single reaction

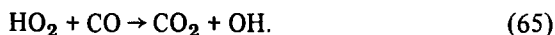
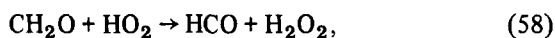
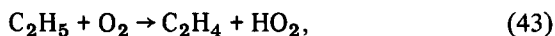
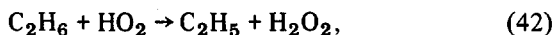
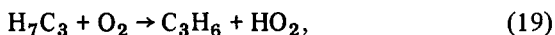
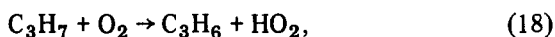
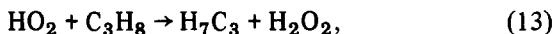
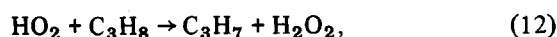
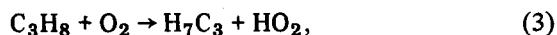
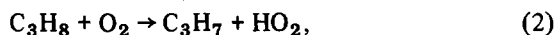


Kanofsky et al. [11] studied the reaction between propylene and the oxygen atom in a low

temperature molecular beam and found that C_2H_5 and HCO are the major products. Similar studies with ethylene showed that CH_3 and HCO are the major products, in agreement with the high temperature results of Peeters and Mahnen [9]. In the present mechanism it was assumed that C_2H_5 and HCO are also the products of the $O + C_3H_6$ reaction at shock tube temperatures in a manner analogous to the $O + C_2H_4$ reaction. In addition, recent work by Baldwin and Walker [12] on the elementary reactions in the oxidation of alkenes revealed that the OH radical also readily reacts with propylene to produce CH_2O and C_2H_5 . Martinez et al. [13] theoretically studied the kinetics of propylene pyrolysis and concluded that other propylene free radical reactions also have an important role in the propylene mechanism. Accordingly, the propylene reaction scheme was expanded to include the following reactions:



Westbrook et al. [34] carried out a numerical study of CO and CH_4 oxidation in a turbulent flow reactor and showed that reactions involving HO_2 and H_2O_2 have an important role in the oxidation process in the temperature range 1000–1350K. Since CH_4 and CO are produced during the combustion of propane, reactions involving the HO_2 radical and H_2O_2 were included in the mechanism. The HO_2 and H_2O_2 reactions that were added to the mechanism not only included the reactions that occur in the H_2 - O_2 system (reactions 73–83) but also reactions involving various hydrocarbon species. The hydrocarbon- HO_2 - H_2O_2 reactions that are in the mechanism include



The rate coefficients assigned to these reactions either were obtained from the literature or were estimated by analogy with similar reactions. The rate coefficients for reactions 2 and 3 were estimated by setting the activation energy equal to the heat of reaction ΔH at 298K and setting the pre-exponential factor at 10^{13} for reaction 2. The pre-exponential factor for reaction 3 was set at one-third the value selected for reaction 2. The one-third factor is the ratio of secondary to primary hydrogens in the propane molecule. Reactions 33, 36, 43, 58, 63, and 65 were included in the mechanism which Westbrook [13, 34] assembled for his numerical studies of methane and ethane oxidation.

MECHANISM EVALUATION

Since many changes and additions were made to the original propane combustion mechanism, it was necessary to compare the observed (experimental) kinetic behavior with that predicted by the mechanism. The experimental data selected for the comparison were the ignition delay times reported by Burcat et al. [3] and the concentration and reaction time data reported by McLain and Jachimowski [1]. Burcat et al. measured ignition delay times in the reflected shock region for propane-oxygen-argon mixtures with equivalence ratios of 0.125–2.0. The temperature range of the experiments was 1150–1650K and the pressures varied from 2 to 14 atm. For the temperature range 1250–1650K the ignition delay time

τ and the mixture composition were correlated through the function

$$\tau[\text{O}_2]^{1.22}[\text{C}_3\text{H}_8]^{-0.57} = 4.4 \times 10^{-8} \exp(44200/RT) \text{ s (mole/cm}^3\text{)}^{0.65}.$$

In several experiments at temperatures lower than 1250K the measured ignition delay times were shorter than predicted by this function. Burcat et al. suggested that this behavior might be due to a change in the mechanism. McLain and Jachimowski [1] studied the combustion of a stoichiometric propane-oxygen-argon mixture behind incident shock waves over the temperature range 1800–2600K. The combustion process was monitored by measuring radiation from carbon dioxide, carbon monoxide, and the reaction $\text{O} + \text{CO} \rightarrow \text{CO}_2 + h\nu$. The recorded emission profiles were analyzed to obtain concentrations for CO_2 , CO , and the product of oxygen atom and the carbon monoxide concentrations.

To compare the kinetic behavior predicted by the mechanism with the experimental results, numerical simulation of the shock tube experiments was carried out using the computer program described by McLain and Rao [32]. To simulate the conditions behind the reflected shock wave, the program was operated in a constant volume mode. Thermochemical data were obtained from the JANNAF tables [35] and Bahn [36]. The rate coefficients for the reverse reactions were calculated within the program using the forward rate coefficient and the appropriate equilibrium constants. Comparisons between the experimental and calculated results are given in Figs. 1–4.

In Fig. 1 a comparison is made between the calculated ignition delay times and the experimental data reported by Burcat et al. for stoichiometric propane-oxygen-argon mixtures. The calculated ignition delay time is defined as it was in the shock tube experiments; that is, it is defined to be the elapsed time between heating of the gas mixture by the reflected shock and the sudden pressure increase due to combustion. Both the experimental and calculated ignition delay times are plotted using the function $\tau[\text{O}_2]^{1.22}[\text{C}_3\text{H}_8]^{-0.57}$, where the ignition delay time is

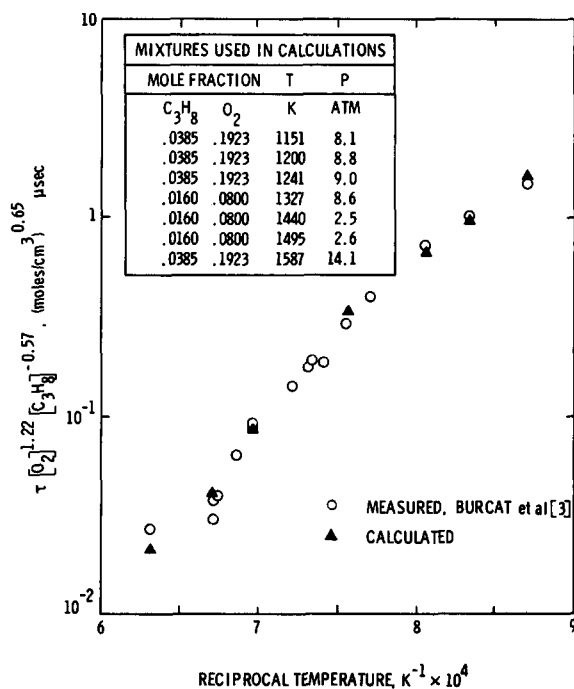


Fig. 1. Comparison of calculated ignition delay times with experimental data reported by Burcat et al. [3] for stoichiometric propane-oxygen-argon mixtures.

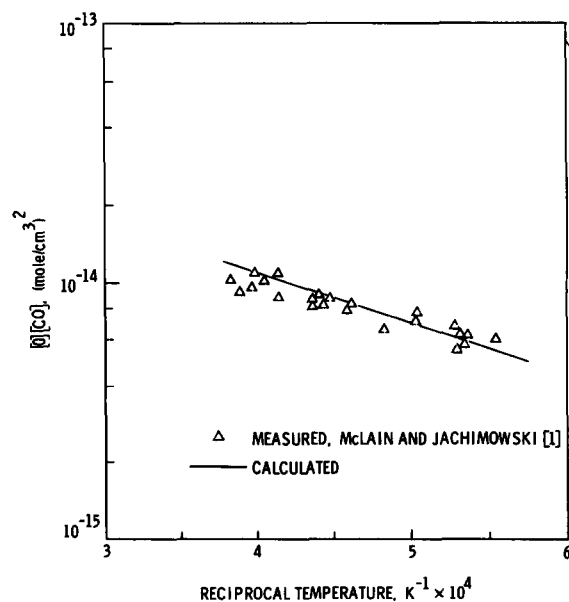


Fig. 2. Comparison of calculated and measured $[\text{O}][\text{CO}]$ values for a 1 mole% C_3H_8 -5 mole% O_2 -94-mole% Ar mixture.

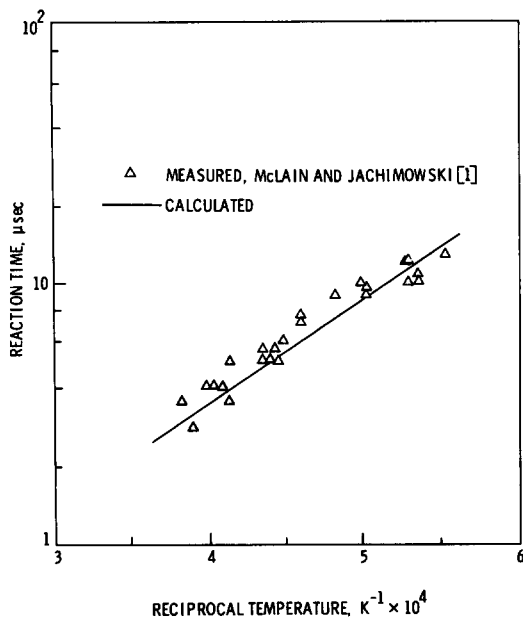


Fig. 3. Comparison of calculated and measured reaction times for a 1 mole% C_3H_8 -5 mole% O_2 -94 mole% Ar mixture.

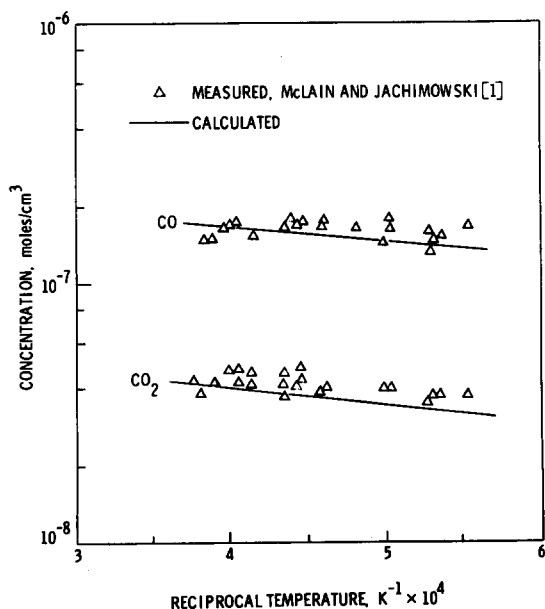


Fig. 4. Comparison of calculated and measured CO and CO_2 concentrations for the 1 mole% C_3H_8 -5 mole% O_2 -94 mole% Ar mixture.

in microseconds and the concentrations are expressed in moles per cm^3 . The calculated results are in very good agreement with the experimental results over the entire temperature range even at temperatures below 1250K, where the increase in ignition delay time with decreasing temperature does not appear to be as large as the increase for temperatures between 1600 and 1500K.

In Figs. 2-4 calculated results are compared with the experimental results reported by McLain and Jachimowski [1] for a 1 mole%-5 mole%-94 mole% argon mixture. The results shown in Fig. 2 are the maximum values of the concentration product $[O][CO]$ that were observed in each experiment and are plotted against the reciprocal of the temperature immediately behind the incident shock wave. Data for reaction time, which is defined as the time interval between the heating of the gas mixture by the incident shock wave and the attainment of the maximum $[O][CO]$ value are shown in Fig. 3. The $[CO]$ and $[CO_2]$ concentration data in Fig. 4 are the observed values at the time of maximum $[O][CO]$. The curves in Figs. 2-4 are the calculated results. The calculated results are in reasonably good agreement with the experimental data. Since the calculated results compared favorably with the experimental results, refinement of the proposed mechanism was not considered necessary and the reactions and rate coefficients listed in Table 1 were used in subsequent theoretical studies. For these studies RRK theory [7] was used to adjust the rate coefficients of unimolecular reactions for the applicable temperature and pressure conditions.

THE KINETICS OF PROPANE COMBUSTION

A series of calculations was made to examine the ignition characteristics of stoichiometric propane-air mixtures over the temperature range 1600-1000K for pressures from 0.5 to 50.0 atm. The purpose of these calculations was to examine more closely the kinetic behavior of propane-air mixtures at the lower temperatures and to determine what effect the HO_2 reactions have on the ignition delay times. The HO_2 radical plays a dominant role in the hydrogen-oxygen reaction particularly at temperatures lower than 1100K and pressures

greater than 1 atm. The role of the HO_2 reactions in the oxidation of propane has not been investigated in great detail, either experimentally or analytically. The proposed propane combustion mechanism contains many hydrocarbon reactions that are involved in the production and/or consumption of the HO_2 radical and H_2O_2 . The rate coefficients assigned to many of these reactions are uncertain to within at least a factor of 10 [15].

Some of the results of the computations are shown in Figs. 5 and 6. In Fig. 5 the ignition delay time is plotted against the reciprocal temperature for pressure ranging from 0.5 to 50 atm. In Fig. 6 the same results are plotted using the correlation function derived by Burcat et al. [3]. The ignition delay time is defined as the time required to achieve ignition as signified by the sudden increase in temperature. The curves in Fig. 5 show that the ignition delay times are more sensitive to temperature than to pressure. For pressures of 1 atm and less, the relationship between $\ln \tau$ and the reciprocal temperature is linear. At higher pressures the relationship becomes more nonlinear, especially for temperatures less than 1200K. For temperatures between 1000 and 1200K and pressures of 5 atm and greater, the ignition delay time increases with decreasing temperature, but to a lesser extent than between 1200 and 1500K. Burcat et al. [3] reported such a trend in the measured ignition delay times in several experiments with stoichiometric propane-oxygen-argon mixtures over the temperature range 1150–1600K. Most of these experiments were conducted at pressures between 8 and 9 atm. They suggested that the trend was real and may indicate a change in the mechanism.

The results shown in Fig. 6 show that the relationship between the correlation function and the reciprocal temperature also becomes nonlinear at pressures larger than 1 atm. Most of the Burcat et al. experiments were run between 1250 and 1600K. For this temperature range the calculations show that the log of the correlation function is linear for pressures between 0.5 and 50 atm.

The shape of the ignition delay time curves for a stoichiometric propane-air mixture at high pressure and low temperatures is opposite to that reported for stoichiometric hydrogen-air mixtures [33]. The effects of temperature and pressure on

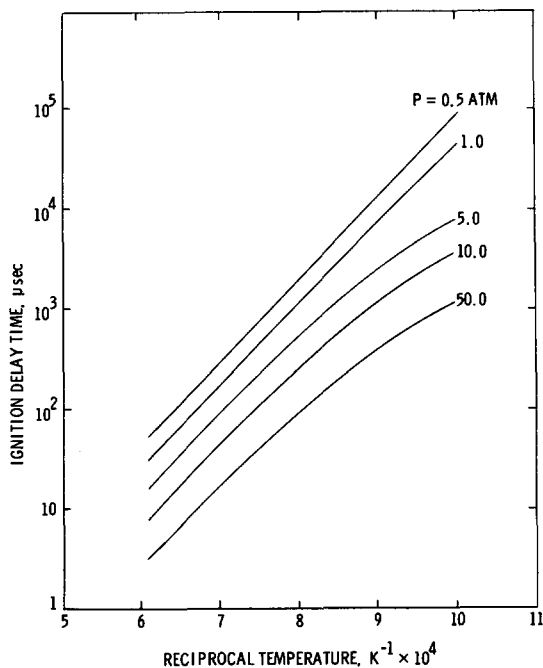


Fig. 5. Ignition times as a function of temperature and pressure for a stoichiometric propane-air mixture.

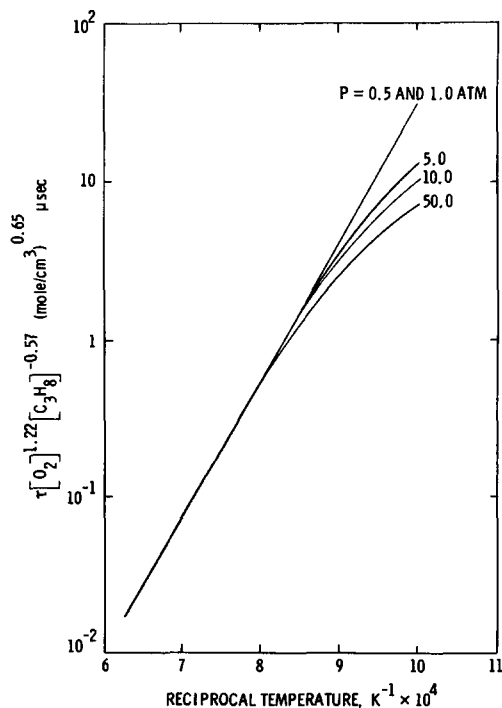


Fig. 6. A plot of the correlation function $\tau[\text{O}_2]^{1.22} [\text{C}_3\text{H}_8]^{0.57}$ as a function of temperature and pressure for the results shown in Fig. 6.

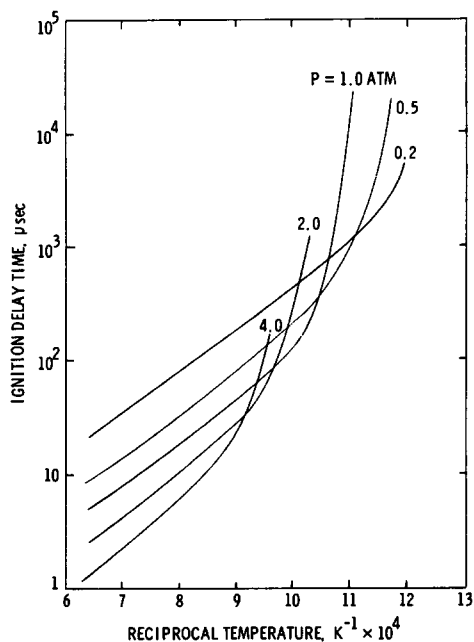


Fig. 7. Ignition delay times as a function of temperature and pressure for a stoichiometric hydrogen-air mixture.

the ignition delay time for a stoichiometric hydrogen-air mixture are shown in Fig. 7. These results were obtained by Rogers and Schexnayder [33], who used a detailed hydrogen-oxygen kinetic mechanism to investigate theoretically the ignition characteristics of hydrogen-air mixtures. In contrast with the results shown in Fig. 5 for propane, the ignition delay time curves for H_2 -air bend upward as the temperature decreases and the pressure increases. This well-known behavior is due to the inhibiting effect of the HO_2 radical, which is kinetically favored at the lower temperatures and higher pressures. Apparently the HO_2 radical does not have a similar effect in the propane-air system for temperatures down to 1000K.

To get a better understanding of the kinetic behavior of the propane-air system at the lower temperatures, a series of calculations was performed in which the sensitivity of the calculated ignition delay times to the rates of various reactions was examined. Special attention was given to the reactions involving the HO_2 radical and H_2O_2 . The sensitivity studies focused on the 3.85 mole% C_3H_8 -19.23 mole% O_2 -76.92 mole% Ar mixture

which Burcat et al. studied experimentally over the temperature range 1150–1587K and pressures between 8 and 14 atm. Most of the calculations were carried out for an initial pressure and temperature of 8.1 atm and 1150K and simulated ignition behind a reflected shock wave (constant volume ignition).

The calculated concentrations of some of the species during the ignition period are plotted in Figs. 8 and 9. The ignition delay time for this mixture is 720 μs and corresponds to the point where the free radical concentrations (H , O , and OH) rapidly increase (see Fig. 8). During the ignition delay period the primary hydrocarbon, propane, is consumed and the principal hydrocarbon products, CH_4 , C_2H_4 , and C_3H_6 , are produced. The concentration of the free radicals H , O , and OH at first increased gradually and then more rapidly as some of the lower molecular weight hydrocarbon products are oxidized. During the period when CH_4 , C_2H_4 , and C_3H_6 are being formed, the levels of the HO_2 radical exceed the levels of the free radicals H , O , and OH . The HO_2 radical concentration decreases rapidly during the

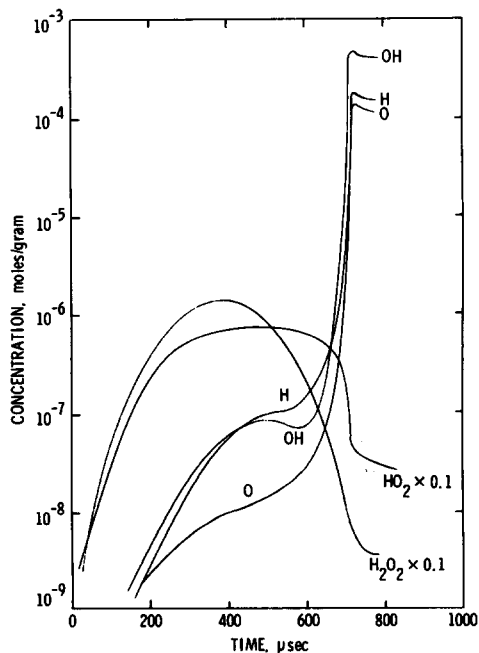


Fig. 8. Calculated concentration profiles during the ignition of a 3.85 mole% C_3H_8 -19.23 mole% O_2 -76.92 mole% Ar mixture initially at 1150K and 8.1 atm.

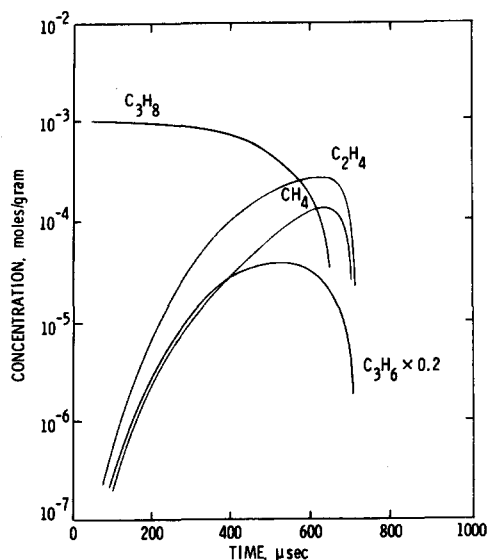


Fig. 9. Calculated hydrocarbon species profiles during the ignition of a 3.85 mole% C_3H_8 -19.23 mole% O_2 -76.92 mole% Ar mixture initially at 1150K and 8.1 atm.

period when the H, O, and OH concentrations rapidly increase. The H_2O_2 levels are also quite high during the ignition delay period and pass through a maximum in a manner similar to the HO_2 concentration.

The results of the sensitivity study revealed that during the ignition delay period propane is primarily consumed by the propagating reactions



with the OH radical being the main abstracting species. The main source of OH radicals during the initial phase ($t < 400 \mu s$) is the homogeneous decomposition of H_2O_2 ,



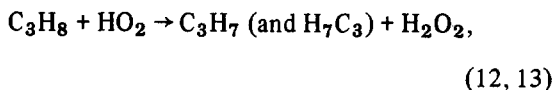
which acts as a source of degenerate chain branching. During the later stages ($400 < t < 650 \mu s$) the reactions



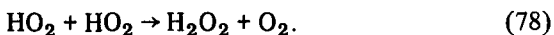
also become important sources of the OH radical. Near the ignition point ($t \cong 700 \mu s$) the chain branching reaction



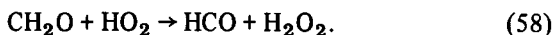
is the primary source of the OH radical. The primary sources of H_2O_2 during the initial stages are the reactions



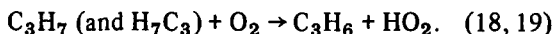
with some contribution from reaction 78,



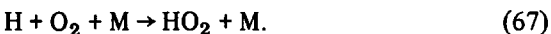
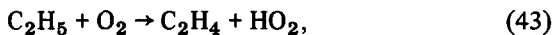
During the later stages of the ignition delay period, when significant levels of CH_2O are produced ($t > 400 \mu s$), reaction 58 also contributes to OH production:



The primary sources of the HO_2 radical during the initial stages are reactions 18 and 19:



Later in the ignition delay period reactions 43 and 67 are the primary sources of the HO_2 radical:



From the results of the sensitivity study it became evident that the HO_2 radical and the H_2O_2 molecule have a major influence on the kinetics of the ignition delay period especially through the hydrocarbon reactions that are involved in the production of HO_2 and H_2O_2 . The importance of the hydrocarbon- HO_2 - H_2O_2 reactions is clearly demonstrated by the results shown in Fig. 10, in which ignition delay times predicted by the mechanism, with and without the hydrocarbon- HO_2 - H_2O_2 reactions, are compared with the experimental results of Burcat

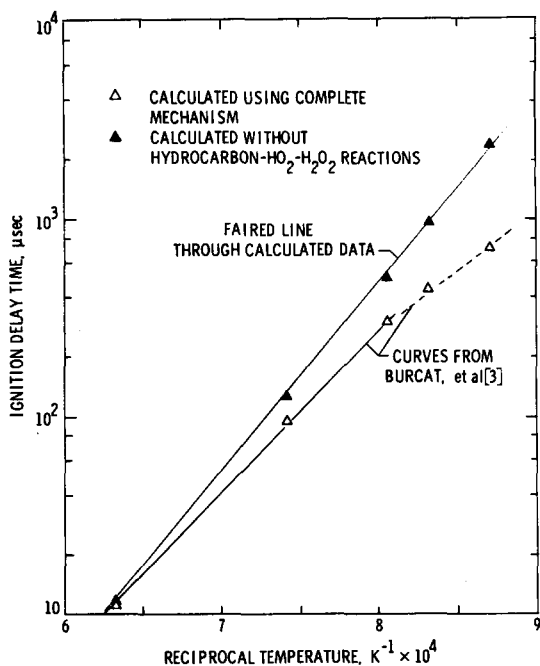


Fig. 10. Calculated ignition delay times compared with experimental data reported by Burcat et al. [3] for the 3.85 mole% C_3H_8 -19.23 mole% O_2 -76.92 mole% Ar mixture.

et al. The reactions that were omitted from the mechanism were reactions 2, 3, 12, 13, 18, 19, 42, 58, 63, and 65. The experimental results are represented by curves derived by Burcat et al. and which are least square fits of the experimental data for the temperature ranges 1250–1587K and 1150–1250K, respectively. The ignition delay times predicted by the complete mechanism are in excellent agreement with the experimental results over the entire temperature range. However, when the hydrocarbon- HO_2 - H_2O_2 reactions are deleted from the mechanism the predicted ignition delay times are longer and exhibit a linear relationship ($\ln \tau$) with the reciprocal temperature. Therefore, the nonlinear behavior of the ignition delay time reported by Burcat et al. appears to be due to the increased importance of the hydrocarbon- HO_2 - H_2O_2 reactions as the temperature is decreased and the pressure is increased.

In conclusion, the propane combustion mechanism presented in Table 1 has been shown to reproduce reasonably the kinetic behavior of

propane-oxygen systems as determined in shock tube studies. The agreement between the predicted and the observed results was achieved without modification of any reaction rate coefficient. The results of analytical studies with the mechanism suggest that hydrocarbon reactions which are involved in the formation of the HO_2 radical and the H_2O_2 molecule become very important at low temperatures. In contrast with the hydrogen-oxygen system, in which the HO_2 radical has an inhibiting effect, the HO_2 radical in the propane-oxygen system is an important chain propagating species.

REFERENCES

1. McLain, A. G., and Jachimowski, C. J., NASA Technical Note D-8501, July 1977.
2. Jachimowski, C. J., and Wilson, C. H., NASA Technical Paper 1794, December 1980.
3. Burcat, A., Lifshitz, A., Scheller, K., and Skinner, G. B., *Thirteenth Symposium (International) on Combustion*, The Combustion Institute, Pittsburgh, 1971, p. 745.
4. Hautman, D. J., Dryer, F. L., Schug, K. P., and Glassman, J., *Combust. Sci. Tech.* 25:293–313 (1981).
5. Chiang, C., and Skinner, G. B., *Eighteenth Symposium (International) on Combustion*, The Combustion Institute, Pittsburgh, 1981, p. 915.
6. Tsang, W., *Ing. J. Chem. Kin.* 1:245 (1969).
7. Golden, D. M., Solly, R. K., and Benson, S. W., *J. Phys. Chem.* 75:1333–1338 (1971).
8. Lifshitz, A., and Frenklach, M., *J. Phys. Chem.* 79: 686–692 (1975).
9. Benson, S. W., and O'Neal, H. E., *Nat. Stand. Ref. Data Ser.*, NBS, No. 21, 1970.
10. Cohen, N., *Int. J. Chem. Kin.* 6:169–228 (1974).
11. Kanofsky, J. R., Lucas, D., and Gutman, D., *Thirteenth Symposium (International) on Combustion*, The Combustion Institute, Pittsburgh 1971, p. 285.
12. Baldwin, R. R., and Walker, R. W., *Eighteenth Symposium (International) on Combustion*, The Combustion Institute, Pittsburgh, 1981, p. 819.
13. Martinez, M., Miller, R. J., and Thommasson, R. L., McDonnell Douglas Report No. G5012, 1974.
14. Westbrook, C. K., *Combust. Sci. Tech.* 20:5–17 (1979).
15. Lloyd, A. C., *Int. J. Chem. Kin.* 6:169–228 (1974).
16. Westley, F., *Nat. Bur. Std. Report* 81-2254, NBS, April 1981.
17. Hartig, R., Troe, J., and Wagner, H. G., *Thirteenth*

- Symposium (International) on Combustion*, The Combustion Institute, Pittsburgh, 1971, p. 147.
18. Tabayashi, K., and Bauer, S. H., *Combust. Flame* 34: 63-83 (1979).
 19. Peeters, J., and Mahnen, G., *Combustion Institute European Symposium*, Academic Press, New York, 1973, p. 53.
 20. Brabbs, T. A., and Brokaw, R. S., *Fifteenth Symposium (International) on Combustion*, The Combustion Institute, Pittsburgh, 1975, p. 893.
 21. Jensen, J., and Jones, G. A., *Combust. Flame* 32:1-34 (1978).
 22. Olson, D. B., and Gardiner, W. C., Jr., *Combust. Flame* 32:151-161 (1978).
 23. Benson, S. W., and Haugen, G. R., *J. Phys. Chem.* 71: 1735-1746 (1967).
 24. Browne, W. G., Porter, R. P., Verlin, J. D., and Clark, A. H., *Twelfth Symposium (International) on Combustion*, The Combustion Institute, 1969, p. 1035.
 25. Dean, A. M., Johnson, R. L., and Steiner, D. C., *Combust. Flame* 3:41-62 (1980).
 26. Jachimowski, C. J., *Combust. Flame* 29:55-66 (1977).
 27. Baulch, D. L., and Drysdale, D. D., *Combust. Flame* 23:215-220 (1974).
 28. Schott, G. L., *Combust. Flame* 21:357-370 (1973).
 29. Gardiner, W. C. Jr., Mallard, W. G., McFarland, M., Morinaga, K., Owen, J. H., Rawlins, W. T., Takeyama, T., and Walker, B. F., *Fourteenth Symposium (International) on Combustion*, The Combustion Institute, Pittsburgh, 1973, p. 61.
 30. Baulch, D. L., Drysdale, D. D., Horne, D. G., and Lloyd, A. G., *Evaluated Kinetic Data for High-Temperature Reactions*, Vol. 1: *Homogeneous Gas Phase Reactions of the H₂-O₂ System*, CRC Press, Cleveland, 1972.
 31. Slack, M. W., *Combust. Flame* 28:241-249 (1977).
 32. McLain, A. G., and Rao, C. S. R., NASA Technical Memorandum X-3403, 1976.
 33. Rogers, R. C., and Schexnayder, C. J., Jr. NASA Technical Paper 1856, 1981.
 34. Westbrook, C. K., Creighton, J., Lund, C., and Dryer, F. L., *J. Phys. Chem.* 81:2542-2554 (1977).
 35. *JANNAF Thermochemical Tables* 2nd ed., NSRDS-NBS 37, U.S. Dept. Commer., 1971.
 36. Bahn, Gilbert S. NASA CR-2178, 1973.

Received 17 June 1983; revised 23 August 1983